Numerical CFD Simulations for Understanding and Optimizing a Biomass Gasifier Reactor Set-Up

E. George[1], J. Nguyen [1],Y. Kara, B[1]. Marchand[1], A. Galnares[1] & [1] O. Guerrini[1]

1. GDF SUEZ, R&D Division - 361, avenue du Président Wilson – 93211 Saint Denis la Plaine Cedex – France

Abstract:
In this paper we present our investigations on biomass used as renewable energy. The numerical study of biomass gasification in fluidized bed was carried out in the framework of the GAYA project supported by ADEME (French Agency For Environmental Protection and Energy). We have developed a sharp expertise in the modeling of the hydrodynamic of simple or multiple phase fluidized beds. Indeed, specific submodels have been developed to represent the particles/particles and fluid/particles interactions. Through our tools we are now able to help in the improvement of an industrial scale gasifier reactor design and analysis.

1. Introduction:

Bioenergy has a substantial potential to substitute fossil energy and alleviate global warming. At the same time, it is a limited resource, which should be used optimally from the environmental perspective. The development of efficient processes for biomass conversion is currently one of the challenges for developing renewable energies in Europe and reach the European goal for a sustainable development. The production of syngas from biomass via steam gasification in a fluidized bed is a very promising technology. The present work deals first with the biomass gasification using the FICFB process. A plant using this technology has been designed and is operated in Austria (Güssing) with a fuel capacity of 8 MW. The goal of this study is to demonstrate the technical relevance and to bring responses to the technological keys of the biomass conversion into BioSNG. The local behavior of the FICFB integration in the process has been studied using a customized version of the commercial CFD ANSYS-Fluent code (such as air supply inlet, freeboard zone on the fluidized bed, expansion of bed, etc.).

2. CFD Modeling Strategy:

The fundamental problem encountered in modeling hydrodynamics of a gas–solids fluidized bed is the motion of the main phases where the interface is unknown and transient, and the interaction is understood only for a limited range of conditions [1]. A first approach is to solve the multi-phase mixture and to treat each phase as continuum media with transfers at the interfaces. However, the mathematical complexities of the non-linear equations and the definition the interpenetrating and moving-phase boundaries make numerical solutions very difficult. With the great advent of increased computational capabilities, CFD is emerging as a very promising new tool in modeling hydrodynamics [2]. While it is now a standard tool for single-phase flows, it is at the development stage for multiphase systems, such as fluidized beds. Work is required to make CFD suitable for fluidized bed reactor modeling and scale-up. Two different approaches have been used in early attempts to apply CFD modeling to gas–solid fluidized beds: a discrete method based on molecular dynamics (Lagrangian model); and a continuous approach based on continuum mechanics treating the two phases as interpenetrating continua (multi-fluid or Eulerian–Eulerian model). In fact it depends on the VOF of dispersed phase(s). The second approach is then used in the present paper.

3. Experimental Rig: Validation Data

The hydrodynamics of a two-dimensional gas–solid fluidized bed reactor were studied both experimentally and computationally. The experimental fluidized bed [3] is a 2D Plexiglas rectangular shape column consisting of spherical glass beads with ambient air as the gas phase. The column dimensions are 0.280 (m) in width, 1.2 (m) in length, and 0.0254 (m) in depth. Ambient air is uniformly injected into the column via a gas distributor which is a perforated plate with a hole to plate cross sectional area ratio of approximately 1.2%.

Pressure drops were measured using three differential pressure transducers located at the elevations of 0.03, 0.3 and 0.6 (m) above the gas distributor. Fig. 1 illustrates the shape of the column used in this research, along with its dimensions and pressure transducer locations. Spherical, non-porous glass beads, Geldart group B particles, with a particle size distribution of 250–300 (μm) and density of 2500 (kg/m^3) were used as the granular parts. The static bed height is 0.4 (m) with a solid volume fraction of approximately
60%. Several experiments were conducted at steady-state bed operations in order to calculate the void fraction and minimum fluidization velocity. In order to estimate the minimum fluidization velocity, measurements were carried out at increasing velocity increments from fixed bed to high inlet velocity (0.6 (m/s)). From the data obtained, minimum fluidization velocity is estimated as
Umf = 0.065 (m/s).

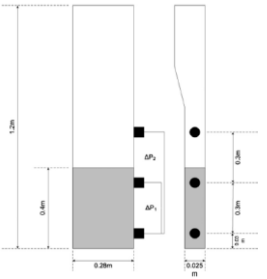

Fig. 1: Geometry of the 2D experimental fluidized bed and transducer locations

The drag force between the gas phase and the particles is one of the dominant forces in a fluidized bed. Generally, drag coefficients, K_{sg}, are obtained from two types of experimental data. The first is for the high value of the solid volume fractions or packed-bed pressure drop data, such as the Ergun drag model. These types of correlations require a complementary drag model for low values of the solid volume fractions, like the Gidaspow drag model. In the second class of data, the terminal velocity of particles in fluidized or settling beds is employed to derive the drag model as a function of void fraction and Reynolds number. An example for this category is the Richardson and Zaki model.

In this paper, six widely used and three much more advanced drag models are used for investigating the modeling of a 2D fluidized bed: Di Felice, Arastoopour, Koch, Wen-yu, Syamlal O'Brien, Richardson & Zaki, modified Syamlal O'Brien[4], Ruc, and BVK [5-6].

4. First CFD : Submodels validation

CFD modeling has been performed using ANSYS-Fluent 13.0. Simulations have been carried out on a 2D fluidized bed using a transient Eulerian–Eulerian model. Several superficial gas velocities, 0.11, 0.21, 0.38, and 0.46 m/s, that correspond to 1.6, 3.2, 5.8, and 7 Umf, respectively, have been studied. In the following section, the simulation results have been compared with the experimental data in order to validate the drag law submodels implemented in the CFD code.

The advanced drag correlations (or submodel) have been implemented in C++ and uploaded in FLUENT as User Defined Functions (UDF).The results have been compared to experimental data in terms of pressure drop and bed expansion ratio .

Fig.2(a) illustrates the computed pressure drop obtained by drag law model deliver in the CFD code release for a 0.38 m/s air velocity.

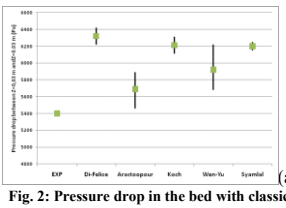

(a)
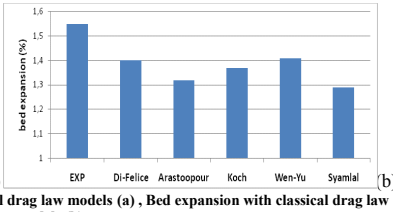

(b)

Fig. 2: Pressure drop in the bed with classical drag law models (a) , Bed expansion with classical drag law models (b)

Expansion of the bed started with formation of bubbles for all the models and eventually reached a statistically steady-state bed height. After this point, an unsteady noise generation of bubbles was observed after almost 3 s of real-time URANS simulation. Fig.2(b) illustrates the computed bed expansion obtained at 0.38 m/s air velocity with classical laws.

It appears that classical drag laws are not suitable for computing the fluidized bed behavior. Our work was then to implement a new (or corrected) law in order to obtain a better representation of the experimental fluidized bed behavior.
Similar results are presented on Fig.3(a) and Fig.3(b).

According to those two last figures, it appears that implemented laws have a better impact on the characterization of global pressure drop and bed expansion for the 0.38 m/s air velocity.

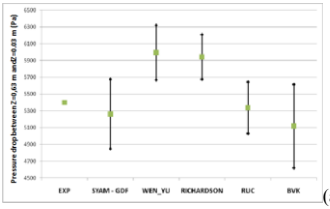

(a)
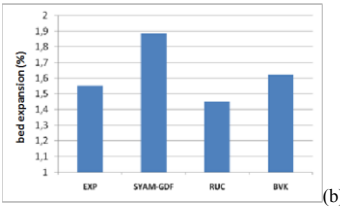

(b)

Fig. 3: Pressure drop in the bed with advanced drag law models (a), Bed expansion with advanced drag law models (b)

Fig. 4 shows a snapshot of solid volume fraction contours for the "best" drag models studied in this work at a superficial gas velocity of 0.38 m/s and after 10 s of real-time URANS simulations.

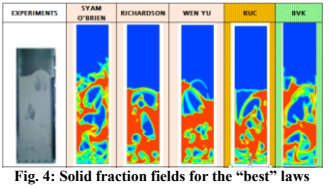

Fig. 4: Solid fraction fields for the "best" laws

In this figure, comparison between all relevant drag models and experimental snapshot has been made in terms of bed height and bubble size and shape. It can be readily observed that the two advanced models RUC and BVK show the best results for simulating the bed height and pressure drop. Nevertheless, the advanced
BVK model is more accurate in the prediction of the bubble shapes and fluctuating behavior of the free surface of the bed.

This is illustrated in Fig. 5(a)-(b) which represent the comparison experiments- BVK for the evolution of both pressure drop and bed expansion in the range of tested air inlet velocities. The time average pressure drop inside the bed between two specific elevations (i.e. 0.03 m and 0.3 m) is calculate by applying both spatial and time averaging.

At first, the spatial averaging, which is the average value of pressure for all nodes in the plane of first pressure transmitter (plane y = 0.03 (m)) has been used. Subsequently, the time averaging of spatial-averaged pressure values in the period of 3–10 (s) real time has been incorporated.

The BVK model is based on extensive lattice-Boltzmann simulations by Van der Hoef et al. [6], and Beetstra et al. [5]. They have proposed expressions for normalized drag force for both mono-dispersed and poly-dispersed systems. Their results found to be in excellent agreement with the simulation data of several models proposed in literatures; the same observation in done here concerning the accuracy of the model [7].

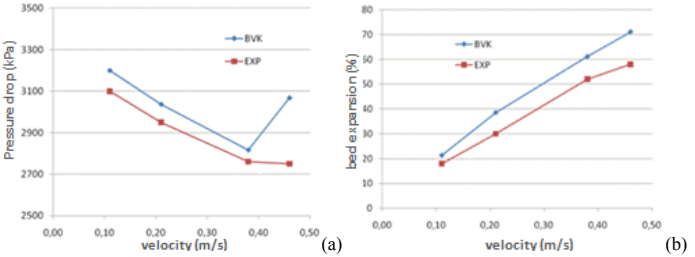

Fig. 5: Pressure drop (0/0.3) vs inlet air velocity(a), Bed expansion vs inlet air velocity (b)

One main advantage of this model is that it is fully adapted to represent a poly-dispersed system as we want to do in our framework.

BVK model has been tested and validated in 2D on the experimental set-up with two solid phases (sand and biomass) and CFD approach in now fully available (drag law, heat transfer (not described here)) and can be used in 3D in order to study more precisely fluidized bed behavior.

5. 3D Results and Discussions:

In this section the 2nd solid phase (biomass or char) behavior in the sand fluidized bed is studied in 3D. The 3D gasifier geometry has been obtained from a previous 2D sketch optimized in term of biomass mixing in the sand fluidized bed (Fig.6).

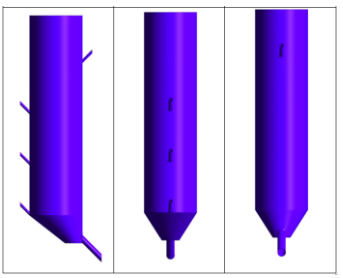

Fig. 6: View of the 3D computational domain

Operating conditions are as follow:

- Inlet air velocity = 1.14 m/s,
- Bed Material – Sand (particle size 275 µm – density = 3040 kg/m^3),
- Initial sand mass = 4.5 kg,
- Sand mass rate = 0.25 kg/s,
- Inlet biomass/char mass rate = 0.0175 kg/s,

- Biomass (particle size 7.5 mm – density = 1040 kg/m^3),
- Char (particle size 0.5 mm – density = 300 kg/m^3).

Then, 4 phases (1 gas phase and 3 solid phases) simulations have been performed during 25 s of real-time URANS simulations on a 7.1 million nodes hexaedrical mesh with 4 CPU (3.3GHz). Computational times do not exceed two weeks.

During the process, the solid phases exit from the bottom of the gasifier due to pressure levels computed in the combustor (not discussed here but also under investigation by the authors).

Three 2nd solid phase injectors locations, illustrated on Fig. 9 have been studied and the middle one has been chosen because it gives the better mixing between sand and char/biomass. Then, a global behavior of such gasifier can be investigated in this configuration.

Fig. 7(a)-(b) show respectively the char history and its impact on sand exit mass flow to the combustor (global mass in the bed and outlet mass flow rate due to combustor conditions).

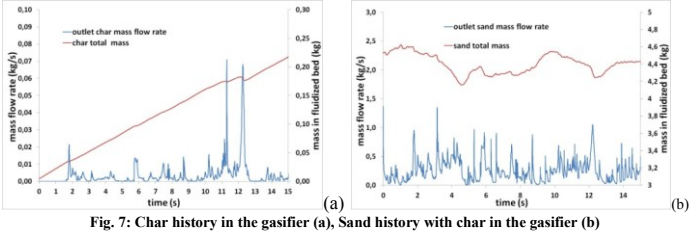

(a) (b)

Fig. 7: Char history in the gasifier (a), Sand history with char in the gasifier (b)

Fig.8 presents the same quantities than Figs.7 but concerning the central biomass injection.

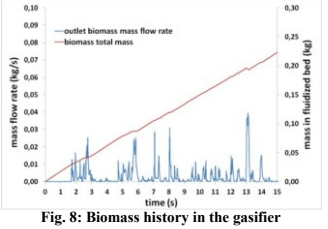

Fig. 8: Biomass history in the gasifier

Fig. 7 to 8 show that the residence time of biomass in the gasifier is higher than the one of the char and then the mass of sand in the gasifier tends to increase.

According to those figures it appears also that the sand behavior at the outlet of the combustor is much more chaotic the one for biomass. This can be explained by the fact that as the computations are for non-reactive conditions, biomass clusters go from the gasifier in the direction of the combustor. Indeed, due to biomass clusters entrainment, the global mass of sand in the gasifier tends to decrease. Those clusters are illustrated on Fig. 9(a) that show both sand and biomass solid fraction after 12 s of real-time URANS simulations.

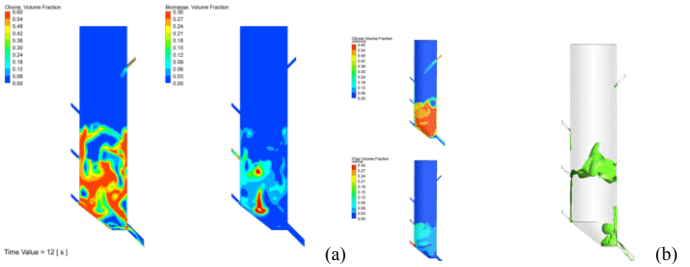

(a) (b)

Fig. 9: Solid fractions field for sand (left) and biomass (right) – cluster formations (a), Hydrodynamic behavior in the gasifier at 3 s: sand (up), char (down) volume fraction (left), and gas bubbling flowpath (right) (b)

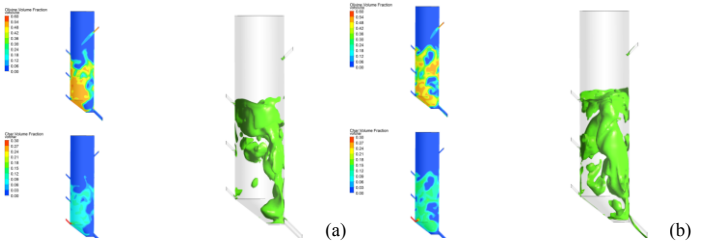

(a) (b)

Fig. 20: Hydrodynamic behavior in the gasifier : sand (up), char (down) volume fraction (left), and gas bubbling flowpath (right) at 6s (a) and 9s (b)

Supprimé: 1

Three different moments are considered from 3 to 12 s of real-time URANS simulations with a 3 s time interval.

3D transient snapshots obtained when computing sand and char (obtained after pyrolysis) hydrodynamic behavior in an industrial scale gasifier are shown in the next figures. Solid fractions are represented with a 0.7 gas fraction that can be useful to estimate the hot gas flow path in the gasifier.

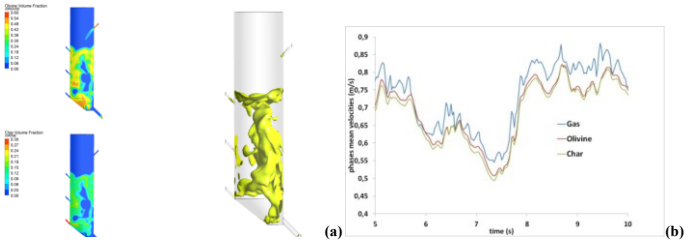

(a) (b)

Fig. 11: Hydrodynamic behavior in the gasifier at 12 s: sand (up), char (down) volumes fraction (left), and gas bubbling flowpath (right) (a), Mean velocities for gas, sand and char (b)

According to Fig. 9 to 11, it appears that the hydrodynamic leads to a preferential flowpath for the fluid into the solid phases. Moreover, the shape of the gasifier's bottom is well adapted to the mixing of the secondary (char) solid phase due to solid recirculation between gas inlet and freeboard zone.

This is confirmed by Fig. 11(b) where both sand and char mean velocities are quite the same after the steady state regime reached at 3 s of real-time URANS simulations.

As we have seen before, the 3 solid phases interaction commands the gasifier global behavior. Classical distribution of residence times method has been adapted to heterogeneous systems and is now perfectly adapted for investigating biomass-char-sand interactions. It has also been shown that the former impact where biomass residence time distribution is higher than those of char is lower in a reacting case when pyrolysis is taken into account: this amount of biomass mass would be less important and char residence time can be very important depending on gasifier internal design. Char behavior is really important for designing the gasifier. Then full reactive case can be studied by transforming biomass into LCV gas (or bio-SNG) and char through the process of devolatilization.
Following Figures show computational rough results of this reacting case.

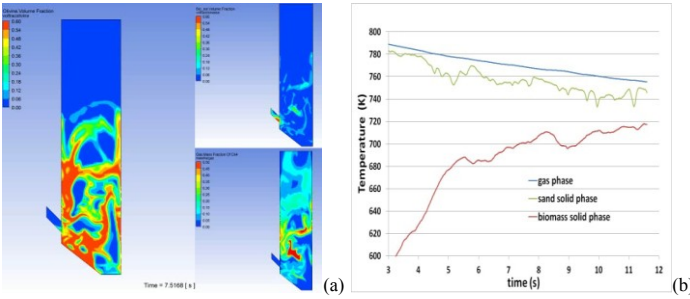

(a) (b)

Fig. 12: Hydrodynamic behavior in the gasifier at 7.5s: sand (left), biomass volumes fraction (up right), and LCV gas mass fraction (down right) (a) and Mean temperature for gas, sand and biomass (b)

Those results have been obtained using a simple and arbitrary conversion model where only temperature leads to the formation of an equivalent LCV gas composition. A kinetic-based model has to be developed in order to estimate as well the impact of biomass residence time and temperature interaction in the conversion process.

All presented model and numerical tools are now validated and available as sub-models in ANSYS-Fluent. They have been used to model the experimental combined GAYA semi-industrial scale gasifier-combustor in order to estimate both design and operating conditions interplay (not discussed here).

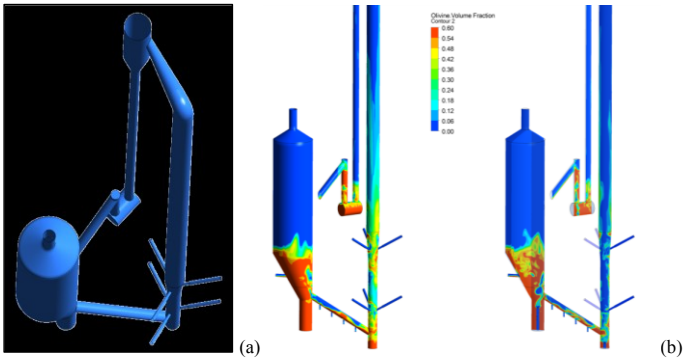

(a) (b)

Fig. 13: Geometry of the gasifier-combustor test facility (a) and associated hydrodynamic behavior of the sand in the gasifier at 40s

6. Conclusion and Outlook:

2D computations have been performed on an experimental set-up to investigate the effect of using different drag correlations for modeling the momentum transfer between phases. The BVK law has been validated and has the advantage to be fully adapted to represent a poly-dispersed system in the targeted conditions.
A validated multi-fluid Eulerian model using ANSYS-Fluent CFD software is then a useful tool to investigate the gas–solid behavior of a fluidized bed.
3D numerical simulation (reacting or not) of a bubbling gas–solid fluidized bed were then performed using the Eulerian–Eulerian approach to investigate the effect of secondary solid phases on the sand fluidized bed hydrodynamic.
Mixing efficiency, defined by biomass injection point, has been optimized using CFD by modifying both geometrical aspects and operation conditions of the gasifier.
According to our design, the char has no real impact on the fluidized bed behavior and is correctly evacuated at the bottom of the gasifier in the direction of the combustion. For biomass, the design tends to increase the quantity of this phase in the gasifier if not the phase change (pyrolysis) is not considered. If so, this point drastically changes with a quasi-steady state achieved.

3D CFD modeling of biomass conversion into bio-SNG and char with a specific kinetic model is the next step of our work.
Developed and implemented models or tools are now available to predict the way of conducting the experimental gasifier of the GAYA Project (location of biomass injection, pressure or temperature captors depending on gasifier operating conditions). Collected data during those tests would be very important to set chemistry properties of the devolatilization process that is purely fundamental and generic here.

7. Acknowledgements:

This study is carried out in the framework of the GAYA project supported by ADEME (French Agency For Environmental Protection and Energy). REPOTEC, an innovative Austrian company which designed the industrial gasifier reactor operated at Güssing, is also a partner of the GAYA project.

8. References

[1] M.A. Gilbertson et al., The motion of particles near a bubble in a gas-fluidized bed, J. of Fluid Mech. **323** (1996) pp377–385
[2] M. Ishii, Thermo-FluidDynamic Theory of Two-Phase Flow. Eyrolles, Paris, (1975)
[3] F. Taghipour et al., Experimental and computational study of gas–solid fluidized bed hydrodynamics. J. of Chem. Eng. Sc. **60** (2005) pp6857-6867
[4] F. Vejahati et al., CFD simulation of gas-solid bubbling fluidized bed: a new method for adjusting drag law, Can. J. of Eng. **87** (2009) pp19-30
[5] R. Beetstra et al., Numerical study of segregation using a new drag force correlation for polydisperse systems derivated from lattice-Boltzmann simulations, Chem. Eng. Sc., **62** (2006) pp246-255
[6] S. Sarkar et al., Fluid-particle interaction from lattice-Botzmann simulations for a flow through polydisperse random arrays of spheres, Chem. Eng. Sc., **64** (2009) pp2683-2691
[7] E. Esnaili et al., Adjustment of drag coefficient correlations in three dimensional CFD simulation of gas–solid bubbling fluidized bed, Adv. Eng. Soft., **42** (2011) pp375-386.